

Detection of a and b waves in the acceleration photoplethysmogram

Mohamed Elgendi^{1,*}

1 Department of Computing Science, University of Alberta, Edmonton, Canada

*** E-mail: moe.elgendi@gmail.com**

Abstract

Analysing photoplethysmogram (PPG) signals measured after exercise is challenging. In this paper, a novel algorithm that can detect a waves and consequently b waves under challenging conditions is proposed. Accurate a and b wave detection is an important first step for the analysis of systolic pressure. Nine algorithms based on fixed thresholding are compared, and a new algorithm is introduced to improve the detection rate. With 27 subjects, the new a detection algorithm demonstrates the highest overall detection accuracy (99.78% sensitivity, 100% positive predictivity) over signals that suffer from 1) non-stationary effects, 2) irregular heartbeats, and 3) low amplitude waves. Moreover, the proposed algorithm presents an advantage for real-time applications by avoiding human intervention in threshold determination. In addition, the proposed b detection algorithm achieved an overall sensitivity of 99.78% and a positive predictivity of 99.95%.

Introduction

Noninvasive pulse-wave analysis has been shown to provide valuable information on aortic stiffness and elasticity [1–3], as it provides more precise information concerning blood pressure changes than systolic and diastolic pressures only [4]. It has been widely used to evaluate the vascular effects of aging, hypertension, and atherosclerosis [5–8]. Photoelectric plethysmography, a common method of pulse-wave analysis, has been referred to as photoplethysmography (PTG/PPG) and digital volume pulse (DVP) analysis; however, the acronym PPG will be used exclusively within this study, according to the recommendations in Ref. [9]. Fingertip photoplethysmography mainly reflects the pulsatile volume changes in the finger arterioles, as shown in Figure 1, and it has been recognized as a noninvasive method for measuring arterial pulse waves in relation to changes in wave amplitude [10]. However, the wave contour

itself has not been analyzed because of the difficulty in detecting minute changes in the phase of the inflections. Previous attempts at PPG analysis showed that such delicate changes in the waves were emphasized and easily quantified by quadratically differentiating the original PPG signal with respect to time [11]. Accordingly, the second derivative of the PPG (SDPPG or APG) was developed as a method that allowed more accurate recognition of the inflection points and easier interpretation of the original plethysmogram wave. The acronym APG will be used exclusively within this study, according to the recommendations in Ref. [9].

As shown in Figure 1, The waveform of the APG consists of four systolic waves (a , b , c , and d waves) and one diastolic wave (e wave) [12]. The height of each wave was measured from the baseline, with the values above the baseline being positive and those under it negative. The relative heights of these waves (b/a , c/a , d/a and e/a ratios), particularly the b/a ratio, has been related to ageing and carotid distensibility [13] and used in calculating the ageing index $(b - c - d - e)/a$ [7]. Recently, the detection of a waves in APG signals has been used to calculate heart rate [14,15] and heart rate variability indexes [16–18].

Although the clinical significance of APG measurement has been well investigated, there is still a lack of studies focusing on the automatic detection of a and b waves in APG signals. However, there was an attempt by Matuyama [19] to find out which of the nine QRS algorithms of Friesens ECG algorithms [20] suits the detection of a waves in APG signals. The detection rate was below 63% for all nine algorithms, even after modifying the thresholds with different values. She concluded her investigation with “a new algorithm should be more robust against noise and should be applicable to both APG and ECG signals”. Therefore, this investigation aimed to develop a robust algorithm to detect a waves in APG signals and to compare its performance with the nine a detection algorithms [19]. Up to the present there has been no attempt to detect b waves in APG signals; and therefore a new method for detecting b wave was introduced. To test the robustness of the developed algorithms, noisy PPG signals (measured at rest and after exercise) were used.

Materials and Methods

Ethics Statement

The PPG data were collected as a minor part of a joint project between Charles Darwin University (Darwin, Northern Territory, Australia), Defence Science and Technology Organisation (DSTO) and the Department of Defence which was initiated by the Department of Defence [19]. The project has been granted human research ethic clearance from Charles Darwin University [19]. Only de-identified numerical data, representing PPG signals as vectors, are stored on the database. The database is available upon request at Charles Darwin University:

<http://www.cdu.edu.au/ehse>.

Database Used

There are currently no standard PPG databases with annotated *a* and *b* waves available to evaluate the developed algorithms. One annotated PPG database is available at Charles Darwin University. The data were measured at rest, after 1 hour of exercise and after 2 hours of exercise, as a minor part of a joint project between Charles Darwin University (Darwin, Australia) and the Department of Defence Science and Technology Organisation. The background of the entire project can be found in Ref. [19]. PPGs of 27 healthy volunteers (males) with a mean \pm SD age of 27 ± 6.9 were measured using a photoplethysmography device (Salus APG, Japan), with the sensor located at the cuticle of the second digit of the left hand. Measurements were taken while the subject was at rest on a chair. PPG data were collected at a sampling rate of 200 Hz. The duration of each data segment was 20 seconds, and an example is shown in Figure 2. For signal conditioning and wave detection, MATLAB 2010b (The MathWorks, Inc., Natick, MA, USA) was used.

Training Set

The PPG signals collected after 1 hour of exercise were used for training as they includes different shapes of PPG waveforms and noise. Moreover, it contained fast rhythm PPG signals, with a total of 885 heart beats, which had an impact on the detection accuracy.

Test Set

PPG signals were measured at rest (before the exercise), with a total of 584 heart beats, and after 2 hours of exercise, with a total of 956 heart beats, were used for testing.

Methodology

In this study, a novel algorithm, adapted from the framework proposed by Elgendi for detecting systolic waves in PPG signals [21] and for detecting QRS complexes in ECG signals [22, 23], will be evaluated. The same approach will be used here to detect the a waves. The method consists of three main stages: pre-processing (bandpass filtering and squaring), feature extraction (generating potential blocks using two moving averages), and classification (thresholding). The structure of the algorithm is given in Figure 3.

Bandpass Filter

A zero-phase second-order Butterworth filter, with bandpass 0.5–15 Hz based on a brute force search that will be discussed later in the parameter optimization section, was implemented to remove the baseline wander and high frequencies that do not contribute to the a wave (cf. Figure 4). The output of the zero-phase Butterworth filter applied to the PPG signal produced a filtered signal $S[n]$, as shown in Figure 5. The code line of this step is line 2 in the pseudocode of the a detection algorithm (Algorithm I).

Second Derivative

To obtain the APG signals, the second derivative was applied to the filtered PPG in order to analyse the APG signals. Equations 1 and 2 represent a non-causal filter; the three-point centre derivative was created with a delay of only two samples.

$$S'[n] = \frac{dS}{dt} \Big|_{t=nT} = \frac{1}{2T}(S[n+1] - S[n-1]), \quad (1)$$

$$Z[n] = \frac{dS'}{dt} \Big|_{t=nT} = \frac{1}{2T}(S'[n+1] - S'[n-1]), \quad (2)$$

where T is the sampling interval and equals the reciprocal of the sampling frequency and n is the number of data points. Figure 5 shows the second derivative of the filtered PPG signal measured at rest and after

exercise. The code line of this step is line 3 in the pseudocode of the a detection algorithm (Algorithm I).

Cancellation of b wave

At this stage, the a wave of the APG needs to be emphasized to distinguish it clearly for detection. This can be done by clipping the negative parts of the APG signal ($Z[n] = 0$, if $Z[n] < 0$). The code line of this step is line 4 in the pseudocode of the a detection algorithm (Algorithm I).

Squaring

Squaring emphasizes the large differences resulting from the a wave, which suppress the small differences arising from the diastolic wave and noise, as shown in Figure 5. This step results in the output

$$y[n] = Z[n]^2, \quad (3)$$

which is important for improving the accuracy in distinguishing the a wave segment in APG signals. The code line of this step is line 5 in the pseudocode of the a detection algorithm (Algorithm I).

Generating Blocks of Interest

Blocks of interest are generated using two event-related moving averages that demarcate the a wave and heartbeat areas. The particular method used to generate blocks of interest has been mathematically shown to detect systolic waves [21] and QRS complexes [22].

In this procedure, the first moving average (MA_{peak}) is used to emphasise the a wave area, as the dotted signal shows in Figure 6, and is given by

$$\text{MA}_{\text{peak}}[n] = \frac{1}{W_1} (y[n - (W_1 - 1)/2] + \dots + y[n] + \dots + y[n + (W_1 - 1)/2]), \quad (4)$$

where W_1 represents the window size of the systolic-peak duration. The resulting value is rounded to the nearest odd integer. The exact value for W_1 of 175 ms is determined after a brute force search, which will be discussed later in the parameter optimization section.

The second moving average (MA_{beat}) is used to emphasize the beat area to be used as a threshold for the first moving average, shown as a dashed signal in Figure 6, and is given by

$$\text{MA}_{\text{beat}}[n] = \frac{1}{W_2}(y[n - (W_2 - 1)/2] + \dots + y[n] + \dots + y[n + (W_2 - 1)/2]), \quad (5)$$

where W_2 represents a window size of approximately one beat duration. Its value is rounded to the nearest odd integer. The exact value for W_2 of 1000 ms is determined after a brute force search, which will be discussed later in the parameter optimization section. The code lines of this step are lines 6–7 in the pseudocode of the a detection algorithm (Algorithm I).

Thresholding

The equation that determines the offset level (α) is $\beta\bar{z}$, where $\beta = 0$ based on a brute force search that will be discussed later in the parameter optimization section, while \bar{z} is the statistical mean of the squared filtered PPG signal. The first dynamic threshold value was calculated by shifting the MA_{beat} signal with an offset level α , as follows:

$$\text{THR}_1 = \text{MA}_{\text{beat}}[n] + \alpha. \quad (6)$$

In this stage, the blocks of interest were generated by comparing the MA_{peak} signal with THR_1 , in accordance with the lines 10–17 the code lines shown in the pseudocode of Algorithm I. Many blocks of interest will be generated, some of which will contain the APG feature (a wave), while others will primarily contain noise. Therefore, the next step is to reject blocks that result from noise. Rejection is based on the anticipated systolic-peak width. In this paper, the undesired blocks are rejected using a threshold called THR_2 , which rejects the blocks that contain diastolic wave and noise. By applying the THR_2 threshold, the accepted blocks will contain a waves only,

$$\text{THR}_2 = W_1. \quad (7)$$

As discussed, the threshold THR_2 corresponds to the anticipated a wave duration. If a block is wider than or equal to THR_2 , it is classified as an a wave. If not, it will be classified as noise. The last stage is to find the maximum absolute value within each block to detect the a wave; the code lines of this step are lines 19–26 in the pseudocode of the a detection algorithm (Algorithm I). Consecutive a waves are shown in Figure 6 to demonstrate the idea of using two moving averages to generate blocks of

interest. Not all the blocks contain potential a waves; some blocks are caused by noise and need to be eliminated. Blocks that are smaller than the expected width for the a wave duration are rejected. The rejected blocks are considered to be noisy blocks and the accepted blocks are considered to contain an a wave. The detected a waves are compared to the annotated a waves to determine whether they were detected correctly. The search range for the true a wave was fixed to ± 50 ms for all algorithms to ensure

consistency of comparison.

Algorithm I: DETECTOR_{aWaves}(PPG_{signal}, F_1 , F_2 , W_1 , W_2 , β)

```

1 :  $a_{\text{waves}} \leftarrow \{\}$ 
2 : Filtered = Bandpass(PPGsignal,  $F_1 - F_2$ )
3 : APG = CentralSecondDerivative(Filtered)
4 : Clipped = Clip(APG)
5 : Qclipped = Square(Clipped)
6 : MApeak = MA(Qclipped,  $W_1$ )
7 : MAbeat = MA(Qclipped,  $W_2$ )
8 :  $\bar{z} = \text{mean}(\mathbf{Q}_{\text{clipped}})$ 
9 :  $\alpha = \beta \bar{z} + \text{MA}_{\text{beat}}$ 
10 : THR1 = MAbeat +  $\alpha$ 
11 : for  $n = 1$  to length(MApeak) do
12 :     if MApeak[ $n$ ] > THR1 then
13 :         BlocksOfInterest[ $n$ ] = 0.1
14 :     else
15 :         BlocksOfInterest[ $n$ ] = 0
16 :     end if
17 : end for
18 : Blocks  $\leftarrow$  onset and offset from BlocksOfInterest
19 : set THR2 =  $W_1$ 
20 : for  $j = 1$  to number of Blocks do
21 :     if width(Blocks[ $j$ ])  $\geq$  THR2 then
22 :          $S_{\text{peaks}} \leftarrow$  index of max. value within the block
23 :     else
24 :         ignore block
25 :     end if
26 : end for
27 : return ( $a_{\text{waves}}$ )

```

Detection of b waves

Figure 7(a) shows the b wave as a global minimum in a subject with good circulation, while Figure 7(b) shows the d wave as a global minimum in a subject with poor circulation [24]. However, in both cases, the b wave is the first minimum after the a wave. The b wave can therefore be detected by finding the local minimum, as follows:

$$(|\mathbf{APG}(a_{\text{waves}}[i] + k)| > |\mathbf{APG}(a_{\text{waves}}[i] + k - 1)|) \wedge (|\mathbf{APG}(a_{\text{waves}}[i] + k)| > |\mathbf{APG}(a_{\text{waves}}[i] + k + 1)|), \quad (8)$$

where \mathbf{APG} is the second derivative of the PPG signal (calculated in line 3 in Algorithm I), i is a counter for the detected a waves, and k is the search interval for the b waves. To reduce the computational complexity for finding b waves, the interval k has been set to vary from 8 ms to 136 ms.

Parameter Optimization

Performance of a wave detection algorithms is typically evaluated using two statistical measures:

$\text{SE} = \text{TP}/(\text{TP} + \text{FN})$ and $\text{+P} = \text{TP}/(\text{TP} + \text{FP})$, where TP is the number of true positives (a wave detected as an a wave), FN is the number of false negatives (a wave has not been detected), and FP is the number of false positives (non- a wave detected as an a wave). The sensitivity SE reported the percentage of true a waves that were correctly detected by the algorithm. The positive predictivity +P reports the percentage of the detected a waves that were true a waves. Similarly, the same statistical measures were used for evaluating the b waves.

The function of the a wave detector (cf. pseudocode of Algorithm I) has five inputs: the PPG signal ($\text{PPG}_{\text{signal}}$), frequency band (F_1 – F_2), event-related durations W_1, W_2 , and the offset (β). Any change in these parameters will affect the overall performance of the proposed algorithm. These parameters are interrelated and cannot be optimized in isolation. A rigorous optimization via brute-force search, over all parameters, was conducted (cf. Table 2). This is a time-consuming process, but it is required before making definitive claims. The data used in this training phase were the PPG signals measured at after 1 hour of exercise. Optimization of the beat detector’s spectral window for the lower frequency resulted in a value within 0.5–1 Hz with the higher frequency within 7–15 Hz. The window size of the first moving average (W_1) varied from 100 ms to 200 ms, whereas the window size of the second moving average

(W_2) varied from 1000 ms to 1.250 s. The offset α was tested over the range 0–10% of the mean value of the squared filtered PPG signal. The QRS complex corresponds roughly to the systolic duration (a wave duration) in APG, which is 100 ± 20 ms in healthy adults [25]. Interestingly, the algorithm uses an optimal value of W_1 (175 ms) corresponded to the a wave duration, and an optimal value of W_2 (1000 ms) for the heartbeat duration. It is clear from Table 2 that the optimal frequency range for the systolic detection algorithm over the database was 0.5–15 Hz. Moreover, the optimal values for the moving-average window sizes and offset are $W_1 = 175$ ms, $W_2 = 1000$ ms, and $\alpha = 0$. The systolic algorithm was adjusted with these optimal parameters. Then, the detector was tested on two PPG datasets (PPG measured at rest and after 2 hours of exercise) without any further adjustment.

Results and Discussion

Based on the parameter optimization step, the value of $\alpha = 0$, which means there is no need for an offset to improve the detection rate, as it was required in detecting QRS in ECG signals [22] and systolic peaks in PPG signals [21]. This is perhaps because of the sharp clear peak (high amplitude) of the a wave compared to the other APG waves (c , d , and e waves).

The a wave detection algorithms were tested on 27 subjects, with the APG signals measured before exercise and after 2 hours of exercise; with a total of 54 recordings. The main objective was to evaluate the robustness of the algorithms against the non-stationary effects, low SNR, and high heart rate exhibited after exercise in conditions of heat stress. Under normal conditions, analyzing stationary APG signals is straightforward; as a waves have similar amplitudes, the statistical characteristics of the signals (i.e., mean and standard deviation) do not change appreciably with time, and a simple threshold level can effectively detect a waves. Figures 8(a) and 9(a) represent the APG signals with stationarity effects for volunteer G2 (before exercise) and L3 (after 2 hours of exercise) (all a waves are almost straight-lined). By contrast, under stress, APG signals become non-stationary, which makes analysis difficult since the standard deviation changes with time (a wave amplitudes vary with time and simple level thresholds cannot optimally detect a waves). This has a negative effect on detection algorithm performance, which is clearly seen in Table 3 when the nine amplitude-dependent algorithms were applied to the APG signals. Moreover, Matsuyama [19] reported that none of the nine amplitude-dependent algorithms achieved acceptable a wave detection rates even after optimizing the threshold values. Most of these nine

algorithms, such as AF2, AF3, FD1, FD2, DF1, and FS1, strictly followed the morphology of the QRS complex. However, it is clear that amplitude-dependent algorithms are not optimal methodologies for detecting a waves in APG signals under varying conditions.

The proposed algorithm scored the highest sensitivity and positive predictivity rates when compared to the nine algorithms. The proposed algorithm appears to be more robust against effects of post-exercise measurement non-stationarity. The results show that the proposed method was able to detect a waves correctly in non-stationary APG signals before exercise, as shown in Figure 8(b), and after 2 hours of exercise, as in Figure 9(b). Moreover, the proposed algorithm was also able to detect a waves correctly in low amplitude APG signals (small voltage), as shown in Figure 8(c), and after 2 hours of exercise, as in Figure 9(c). However, the algorithm did incur a few instances of failure, with exactly five FNs, as shown in Table 3. The cause of the failure was due to the sudden drop in amplitude of the a waves in heat-stressed APG signals (cf. Figure 10). The proposed method, however, handled varying amplitudes well compared to the other nine algorithms. In fact, it is clear that the proposed algorithm is more amplitude-independent and was able to detect the a waves in various voltage ranges.

The analysis of a regular heart rhythm is simple, as the a waves are repeated with an equally spaced pattern. This regularity helps the time-domain threshold methodologies to detect a waves successfully. The regular heart rhythm is called the normal sinus rhythm in APG signals [26], which means the rhythm is constant and the occurrence of the next beat is predictable. The proposed algorithm easily detects a waves correctly in APG signals with a regular heart rhythm, as shown in Figure 8(a,b,c). The sensation of an irregular heart rhythm is usually related to either premature beats or atrial fibrillation. The proposed algorithm also successfully detected the a waves with premature beats in both conditions at rest and after exercise, as shown in Figures 8(d) and 9(d).

As the detection of b waves depends on the detection of a waves, the performance of the b wave detection scored almost the same result as the a detection algorithm. Because the proposed b detection incurred only one instance of failure, which is a TP shown in Figure 10, the +P becomes 99.95%. This result reflects the robustness of the proposed b detection algorithm against noisy APG signals.

Limitations of the Study and Future Work

One of the next steps regarding the results of this study is to examine the correlation of the a/b ratio (based on the accurately detected a and b waves) using APG signals with age, body mass index, and core temperature. Moreover, there is a need for developing an algorithm that detects the c , d , and e waves.

It is important to note that the number of PPG records (total of 27) used in the training was modest. A larger sample size and a more diverse data set are needed in order to generalize the findings of this study. The evaluation of a wave detection was challenging in this study because the number of annotated beats did not allow all possible morphologies found in APG signals under conditions of heat stress to be well represented. To our knowledge, there is no available APG database measured after heat stress that would allow a more thorough assessment and comparison of the tested algorithms.

Technically, the event-related moving average methodology for detecting events in APG signal is promising in terms of computational complexity and efficiency. This can be further improved by investigating other bandpass filters, with different orders, and also by developing fast moving average techniques for real-time analysis and mobile phone applications.

Conclusion

For all nine QRS algorithms, the detection errors arose from a variety of factors including the existence of irregular heartbeats, low-amplitude peaks, and signals with non-stationary effects. The application of an event-related dual moving average would allow the accurate, computationally simple algorithm we propose to be used for real-time applications and the processing of large databases. A detection algorithm for a waves in APG signals measured after exercise has not been previously addressed in the literature, with the exception of Matsuyam's thesis. However, it has been demonstrated that a robust algorithm can be developed for detecting a waves in APG signals collected in a noisy environment with high-frequency noise, low amplitude, non-stationary effects, irregular heartbeats, and high heart rates. The a wave detection algorithm was evaluated using 27 records, containing 1,540 heartbeats (584 heartbeats measured at rest and 956 heartbeats measured after 2 hours of exercise), with an overall sensitivity of 99.78%, and the positive predictivity was 100%, while the b detection algorithm scored an overall sensitivity of 99.78% and a positive predictivity of 99.95%.

Acknowledgments

Mohamed Elgendi would like to gratefully acknowledge the Australian government and Charles Darwin University, as their generous scholarships facilitated this research. He appreciates the support of Prof. Friso De Boer, who provided access to the PPG database and valuable comments, and acknowledges Dr. Gari Clifford for the helpful discussions.

References

1. Chrife R, Pigott V, Spodick D (1971) Measurement of the left ventricular ejection time by digital plethysmography. *American Heart Journal* 82: 222–227.
2. Kelly R, Hayward C, Avolio A, O'Rourke M (1989) Noninvasive determination of age-related changes in the human arterial pulse. *Circulation* 80: 1652–1659.
3. O'Rourke M, Avolio A, Kelly R (1992) *The Arterial Pulse*. Baltimore: Lea & Febiger.
4. Takazawa K, Tanaka N, Takeda K, Kurosu F, Ibukiyama C (1995) Underestimation of vasodilator effects of nitroglycerin by upper limb blood pressure. *Hypertension* 26: 520–523.
5. Darne B, Girerd X, Safar M, Cambien F, Guize L (1989) Pulsatile versus steady component of blood pressure: a cross-sectional analysis and a prospective analysis on cardiovascular mortality. *Hypertension* 13: 392–400.
6. Barenbrock M, Spieker C, Kerber S, Vielhauer C, Hoeks A, et al. (1995) Different effects of hypertension, atherosclerosis and hyperlipidemia on arterial distensibility. *Hypertension* 13: 1712–1717.
7. Takazawa K, Tanaka N, Fujita M, Matsuoka O, Saiki T, et al. (1998) Assessment of vasoactive agents and vascular aging by the second derivative of photoplethysmogram waveform. *Hypertension* 32: 365–370.
8. Bortolotto A, Jacques B, Takeshi K, Kenji T, Michel S (2000) Assessment of vascular aging and atherosclerosis in hypertensive subjects: second derivative of photoplethysmogram versus pulse wave velocity. *American Journal of Hypertension* 13: 165–171.

9. Elgendi M (2012) Standard terminologies for photoplethysmogram signals. *Current Cardiology Reviews* 8: 215–219.
10. Fitchett D (1984) Forearm arterial compliance: a new measure of arterial compliance? *Cardiovascular Research* 18: 651–656.
11. Seki H (1977) Classification of wave contour by first and second derivative of plethysmogram (in japanese). *Pulse Wave* 7: 42-50.
12. Takazawa K, Fujita M, Kiyoshi Y, Sakai T, Kobayashi T, et al. (1993) Clinical usefulness of the second derivative of a plethysmogram (acceleration plethysmogram). *Cardiology* 23: 207–217.
13. Imanaga I, Hara H, Koyanagi S, Tanaka K (1998) Correlation between wave components of the second derivative of plethysmogram and arterial distensibility. *Jpn Heart J* 39: 775–784.
14. Taniguchi K, Nishikawa A, Nakagoe H, Sugino T, Sekimoto M, et al. (2007) Evaluating the surgeon's stress when using surgical assistant robots. pp. 888–893.
15. Elgendi M, Jonkman M, De Boer F (2009) Measurement of $a-a$ intervals at rest in the second derivative plethysmogram. In: the IEEE 2009 International Symposium on Bioelectronics and Bioinformatics, RMIT University, City Campus Melbourne, Australia. pp. 75–79.
16. Elgendi M, Jonkman M, De Boer F (2010) Applying the APG to measure heart rate variability. In: the 2nd International Conference on Computer and Automation Engineering, Singapore. pp. 100–104.
17. Elgendi M, Jonkman M, De Boer F (2010) Heart rate variability measurement using the second derivative photoplethysmogram. In: the 3rd International Conference on Bio-inspired Systems and Signal Processing (BIOSIGNALS2010), Valencia, Spain. pp. 82–87.
18. Elgendi M, Jonkman M, De Boer F (2011) Heart rate variability and acceleration plethysmogram measured at rest. In: Fred A, Filipe J, Gamboa H, editors, *Biomedical Engineering Systems and Technologies*, Springer, Communications in Computer and Information Science. pp. 266–277.
19. Matsuyama A (2009) ECG and APG Signal Analysis during Exercise in a Hot Environment. PhD Thesis, Charles Darwin University, Darwin, Australia.

20. Friesen GM, Jannett TC, Jadallah MA, Yates SL, Quint SR, et al. (1990) A comparison of the noise sensitivity of nine QRS detection algorithms. *IEEE Trans Biomedical Engineering* 37: 85-98.
21. Elgendi M, Norton I, Brearley M, Abbott D, Schuurmans D (2013) Systolic peak detection in acceleration photoplethysmograms measured from emergency responders in tropical conditions. *PLoS ONE*. doi:10.1371/journal.pone.0076585. In press.
22. Elgendi M (2013) Fast QRS detection with an optimized knowledge-based method: evaluation on 11 standard ECG databases. *PLoS ONE*. doi:10.1371/journal.pone.0073557. In press.
23. Elgendi M, Jonkman M, De Boer F (2010) Frequency bands effects on QRS detection. In: the 3rd International Conference on Bio-inspired Systems and Signal Processing (BIOSIGNALS2010). pp. 428–431.
24. Elgendi M (2012) On the analysis of fingertip photoplethysmogram signals. *Current Cardiology Reviews* 8: 14–25.
25. Clifford GD, Azuaje F, McSharry P (2006) *Advanced Methods and Tools for ECG Data Analysis*. London: Artech House Publishers, 1st edition.
26. Braunwald E, Zipes D, Libby P, Bonow R (2004) *Braunwald's Heart Disease: A Textbook of Cardiovascular Medicine*. Philadelphia: Saunders, 7th edition.

Tables

Table 1. A rigorous optimization over all parameters of the a wave detection algorithm: frequency band, W_1 , W_2 , and the offset β . All possible combinations of parameters (5,610 iterations) have been investigated and sorted in descending order according to their overall accuracy. The data used in this training phase were PPG measured after 1 hour of exercise, with 885 heartbeats. The overall accuracy is the average value of SE and +P.

Iterations	Frequency Band	W1	W2	Offset (%)	SE (%)	+P (%)	Overall Accuracy (%)
1	0.5-15 Hz	35	200	0	99.72	100.00	99.86
2	0.5-11 Hz	25	200	0	99.92	99.78	99.85
3	1-15 Hz	35	200	0	99.68	100.00	99.84
4	0.5-13 Hz	35	200	0	99.67	100.00	99.84
5	0.5-14 Hz	20	220	0	100.00	99.64	99.82
6	1-14 Hz	35	200	0	99.64	100.00	99.82
7	0.5-14 Hz	20	200	0	99.92	99.71	99.82
8	0.5-14 Hz	20	210	0	99.92	99.71	99.82
9	0.5-13 Hz	25	200	0	99.84	99.78	99.81
10	1-14 Hz	25	200	0	99.84	99.78	99.81
11	1-14 Hz	25	210	0	99.84	99.78	99.81
12	0.5-13 Hz	20	200	0	99.92	99.66	99.79
13	1-15 Hz	30	200	0	99.75	99.82	99.79
14	0.5-15 Hz	30	200	0	99.68	99.89	99.78
15	1-9 Hz	35	200	0	99.55	100.00	99.78
16	0.5-12 Hz	25	220	0	100.00	99.55	99.78
17	0.5-14 Hz	35	200	0	99.54	100.00	99.77
18	1-15 Hz	30	250	0	99.75	99.79	99.77
19	0.5-15 Hz	25	200	0	99.92	99.61	99.76
20	0.5-12 Hz	25	200	0	99.84	99.68	99.76
•	•	•	•	•	•	•	
•	•	•	•	•	•	•	
•	•	•	•	•	•	•	
5606	0.5-8 Hz	40	230	10	90.22	99.88	95.05
5607	0.5-7 Hz	40	230	9	89.80	99.88	94.84
5608	0.5-7 Hz	40	240	9	89.96	99.68	94.82
5609	0.5-7 Hz	40	230	10	89.21	99.88	94.55
5610	0.5-7 Hz	40	240	10	89.38	99.68	94.53

Table 2. Performance of the proposed a wave detection algorithm on the testing dataset (APG signals measured at rest and after 2 hours of exercise). The PPG signals were collected from 27 subjects for 20 seconds during the 5 minutes break between each exercise [19]. To compare the performance of the proposed algorithm with the nine algorithms [19], two statistical measures were used: $SE = TP/(TP + FN)$ and $+P = TP/(TP + FP)$, where TP is the number of true positives (a wave detected as a wave), FN is the number of false negatives (a wave has not been detected), and FP is the number of false positives (non- a wave detected as a wave).

Record	Before Exercise						After 2 Hours of Exercise					
	No of beats	TP	FP	FN	Se (%)	+P (%)	No of beats	TP	FP	FN	Se (%)	+P (%)
A1	26	26	0	0	100	100	43	41	0	2	95.34	100
A2	24	24	0	0	100	100	47	47	0	0	100	100
B1	17	17	0	0	100	100	44	43	0	1	97.72	100
B2	26	26	0	0	100	100	38	38	0	0	100	100
C2	20	20	0	0	100	100	37	37	0	0	100	100
C3	20	20	0	0	100	100	23	23	0	0	100	100
D2	22	22	0	0	100	100	39	39	0	0	100	100
D3	19	19	0	0	100	100	27	27	0	0	100	100
E1	22	22	0	0	100	100	30	30	0	0	100	100
E2	22	22	0	0	100	100	30	30	0	0	100	100
E3	19	19	0	0	100	100	38	38	0	0	100	100
G2	30	30	0	0	100	100	49	48	0	1	97.95	100
G3	19	19	0	0	100	100	42	41	0	1	97.61	100
H3	23	23	0	0	100	100	32	32	0	0	100	100
I1	22	22	0	0	100	100	35	35	0	0	100	100
I2	17	17	0	0	100	100	31	31	0	0	100	100
J2	23	23	0	0	100	100	41	41	0	0	100	100
L2	24	24	0	0	100	100	37	37	0	0	100	100
L3	24	24	0	0	100	100	39	39	0	0	100	100
N2	18	18	0	0	100	100	24	24	0	0	100	100
N3	20	20	0	0	100	100	31	31	0	0	100	100
O1	24	24	0	0	100	100	33	33	0	0	100	100
O2	17	17	0	0	100	100	34	34	0	0	100	100
P1	26	26	0	0	100	100	34	34	0	0	100	100
P2	20	20	0	0	100	100	34	34	0	0	100	100
Q1	22	22	0	0	100	100	28	28	0	0	100	100
Q2	18	18	0	0	100	100	36	36	0	0	100	100
²⁷ volunteers	584	584	0	0	100	100	956	951	0	5	99.57	100

Table 3. Comparison of different a wave detection performance on the testing dataset (APG signals measured at rest and after 2 hours of exercise). The PPG signals were collected from 27 subjects for 20 seconds during the 5 minutes break between each exercise [19]. To compare the performance of the proposed algorithm with the nine algorithms [19], two statistical measures were used: $SE = TP/(TP + FN)$ and $+P = TP/(TP + FP)$, where TP is the number of true positives (a wave detected as a wave), FN is the number of false negatives (a wave has not been detected), and FP is the number of false positives (non- a wave detected as a wave). Here, NA stands for Not Applied, while NaN stands for Not-a-Number.

Algorithm	TP (%)	FN (%)	FP (%)	Se (%)	+P (%)	Threshold Values		
						THR ₁	THR ₂	THR ₃
Proposed algorithm	100	0.32	0	99.78	100	$MA_{\text{beat}} + \alpha$	W_2	NA
AF1 [19]	69.5	7.5	30.5	90.25	69.5	0.31	0.0001	-0.001
AF2 [19]	0.018	0.27	99.98	6.25	0.018	0.21	0.75	NA
AF3 [19]	0	0	100	NaN	0	62	NA	NA
FD1 [19]	0.27	2.8	99.73	8.79	0.27	0.099	NA	NA
FD2 [19]	0	0	100	NaN	0	150	NA	NA
DF1 [19]	0	0	100	NaN	0	21	NA	NA
DF2 [19]	48.8	14.2	51.2	77.46	48.8	1	0.06	NA
FS1 [19]	2.42	0.3	97.58	88.97	2.42	154.5	NA	NA
FS2 [19]	42.46	6.9	57.54	86.02	42.46	0.55	0.47	NA

Figures

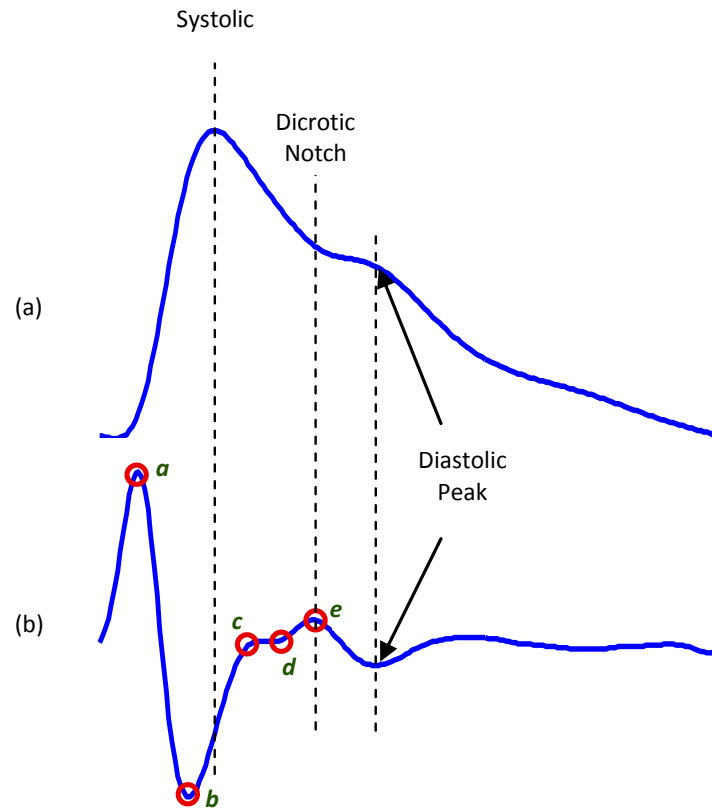


Figure 1. Fingertip photoplethysmogram signal measurement [24]. (a) Fingertip photoplethysmogram. (b) Second derivative wave of photoplethysmogram. The photoplethysmogram waveform consists of one systolic wave and one diastolic wave, while the second derivative photoplethysmogram waveform consists of four systolic waves (*a*, *b*, *c*, and *d* waves) and one diastolic wave (*e* wave).

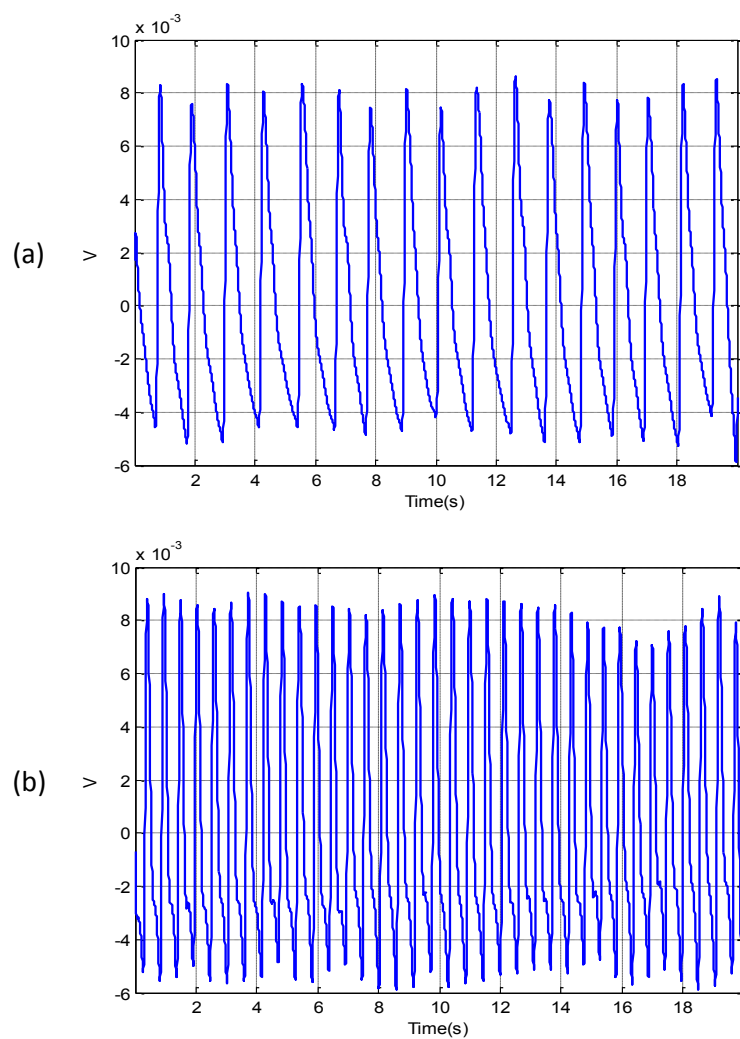


Figure 2. An example of PPG recordings for the same volunteer measured (a) at rest and (b) after exercise. It is clear that the heart rate after exercise was higher than at rest.

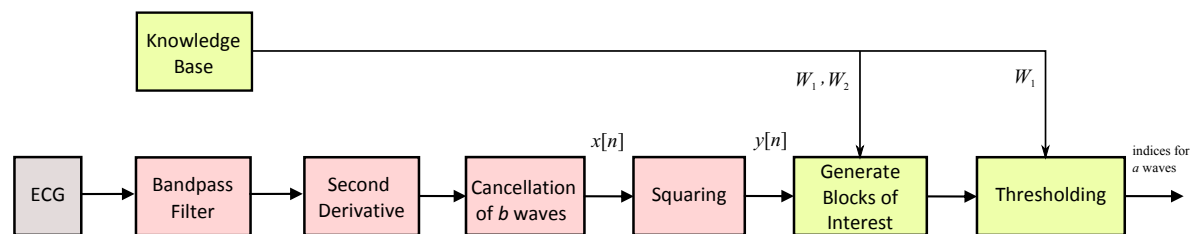


Figure 3. Flowchart of the knowledge-based a wave detection algorithm. The algorithm consists of three stages: pre-processing (bandpass filter, cancellation of b waves, and squaring), feature extraction (generating blocks of interest based on prior knowledge), and thresholding (based on prior knowledge).

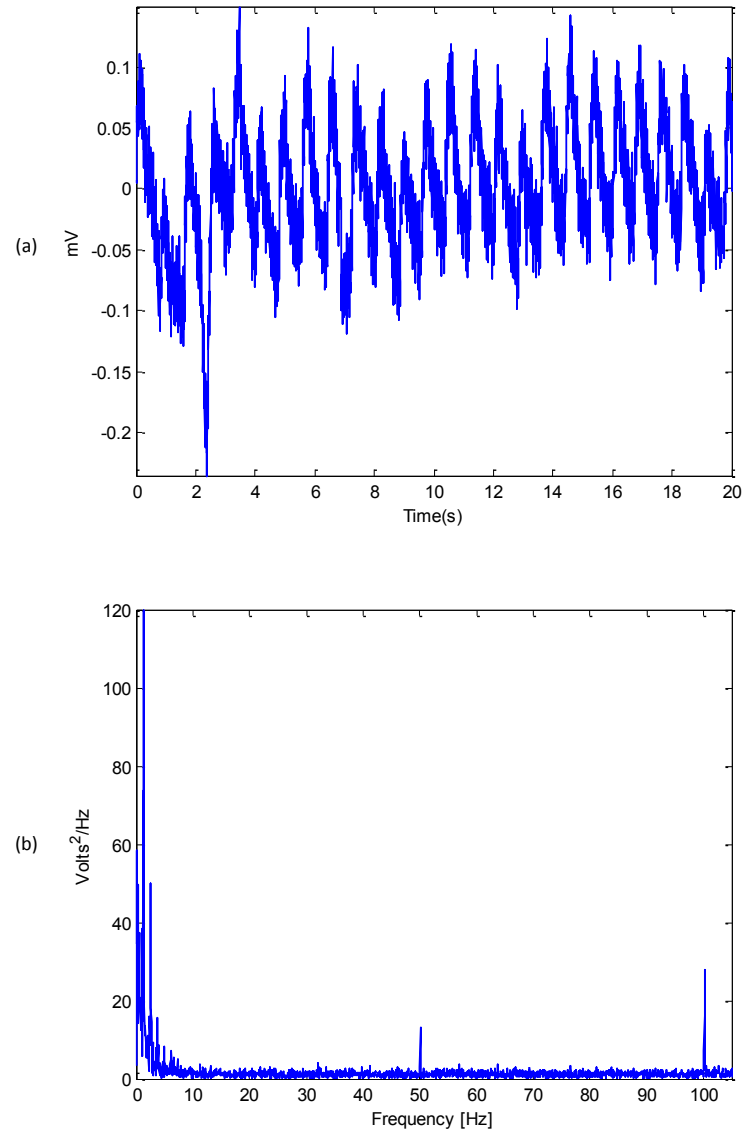


Figure 4. Fourier transform of noisy PPG signals: (a) PPG signal and (b) Fourier transform (spectrum) of the PPG signal. The spectrum illustrates peaks at the fundamental frequency of 50 Hz, as well as the second and third harmonics at 100 Hz. The spectrum shows that the main energy of the PPG signal lies below 20 Hz.

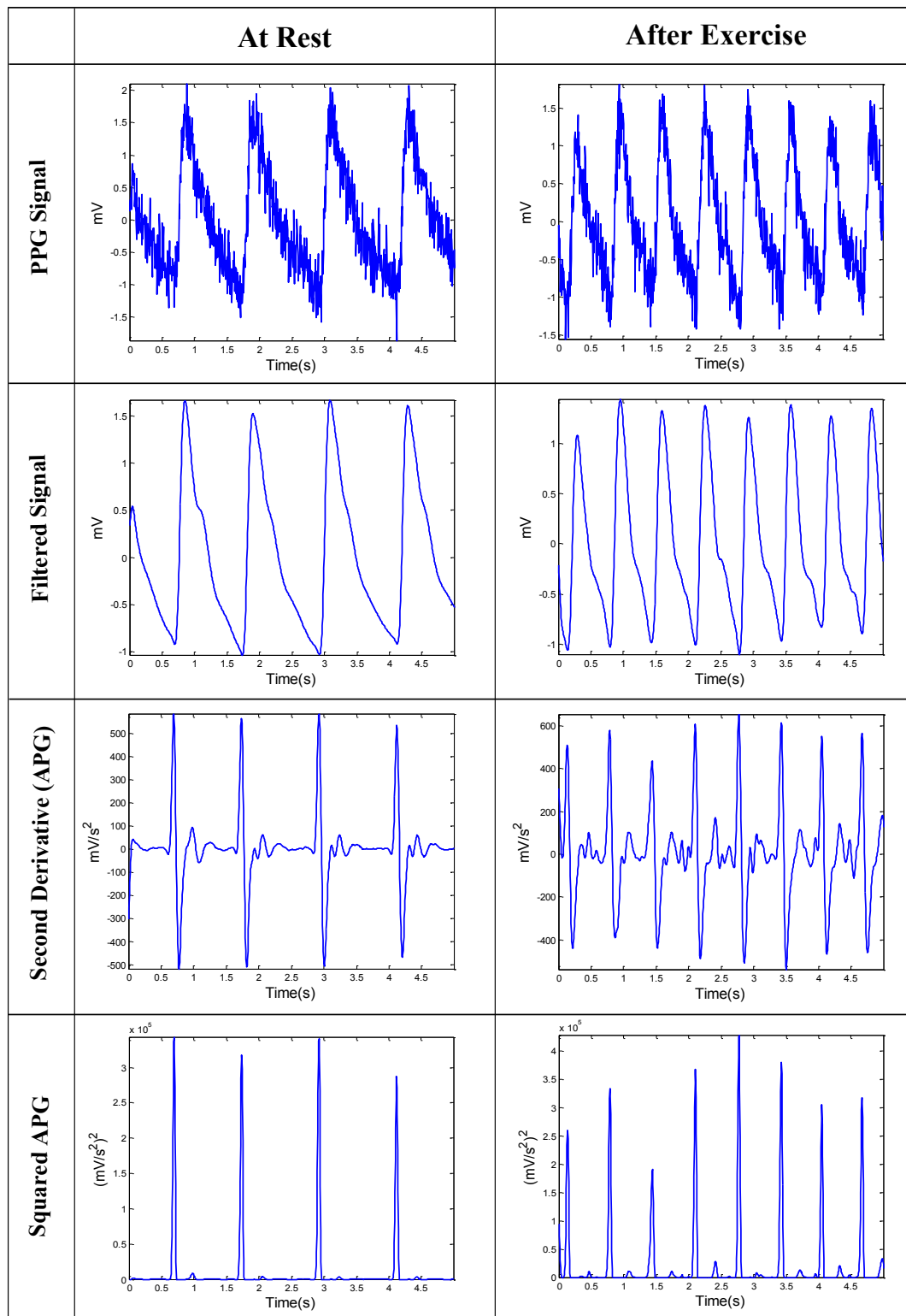


Figure 5. The proposed algorithm output for PPG measured at rest and after exercise.

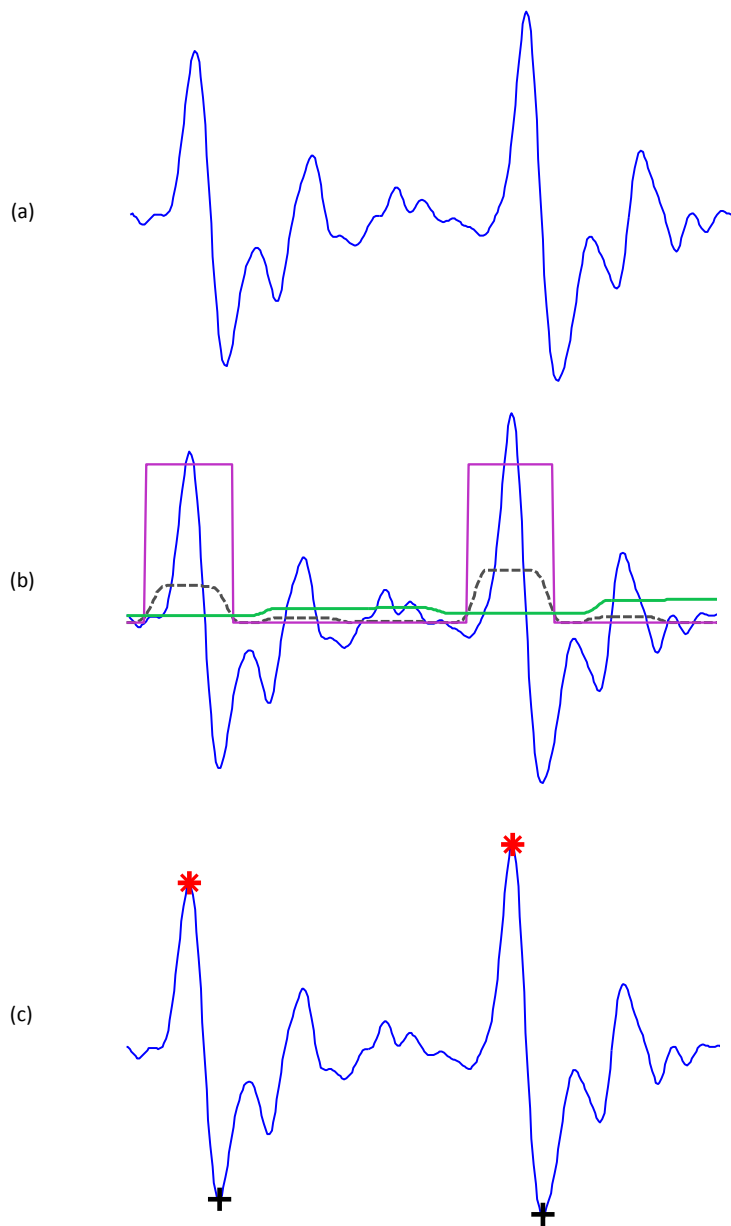


Figure 6. Demonstrating the effectiveness of using two moving averages to detect *a* and *b* waves. (a) Two beats APG signal; (b) generating blocks of interest after using two moving averages: the dotted black line is the first moving average MA_{peak} and the solid green line is the second moving average MA_{beat} ; and (c) the detected *a* and *b* waves after applying the thresholds.

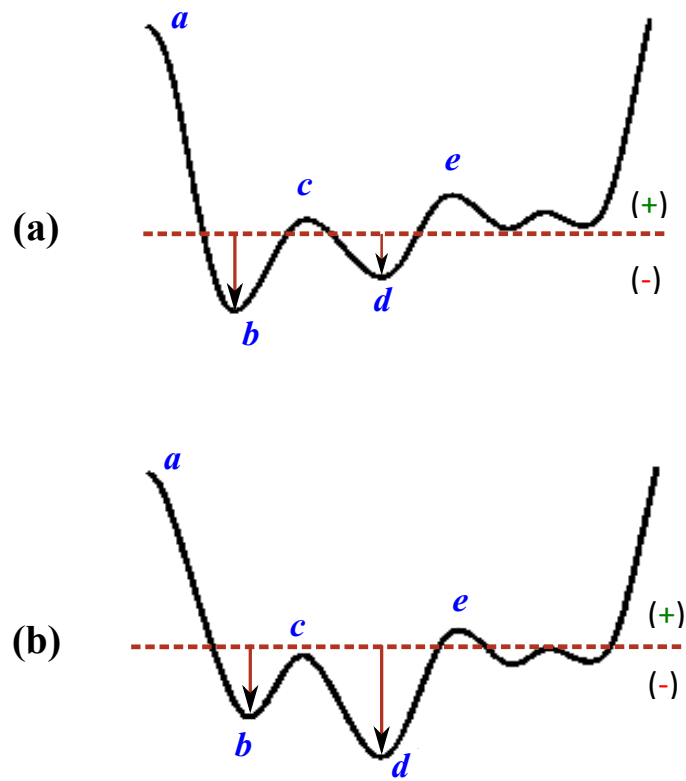


Figure 7. Demonstrating the local minimum and global minimum of the *b* wave in the APG signal. (a) *b* wave is global minimum, (b) *b* wave is local minimum.

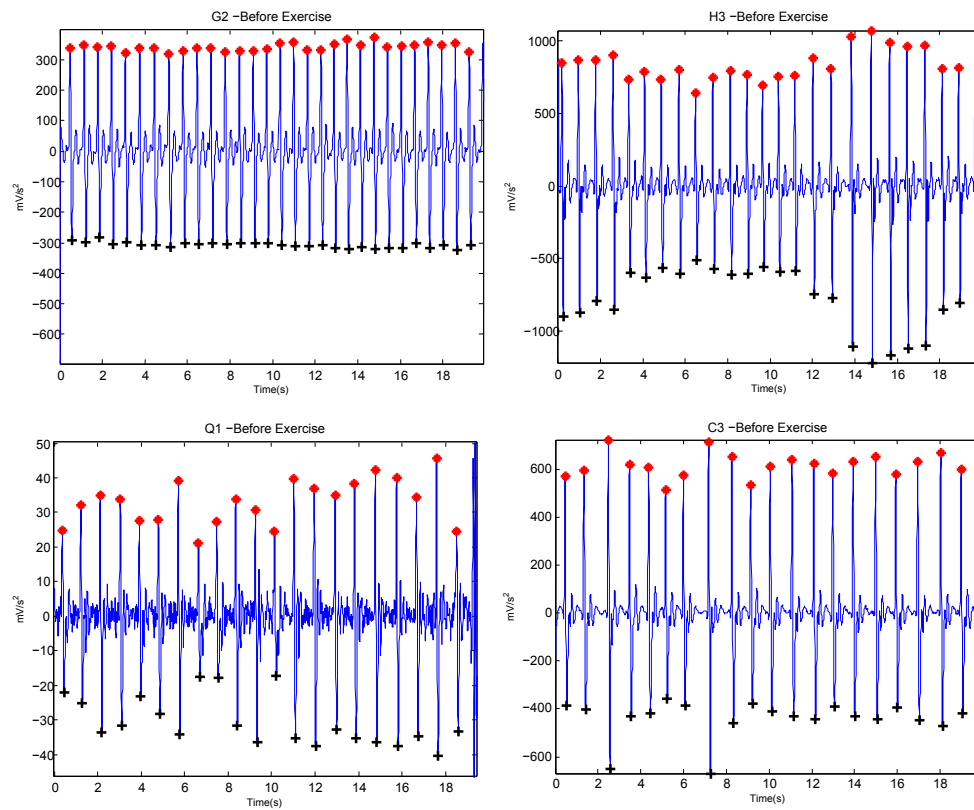


Figure 8. Detected a and b waves in APG signals at rest (before exercise). It contains (a) stationary signals, (b) non-stationary signals, (c) low amplitudes, and (d) irregular heart rhythm. Here, ‘*’ represents the detected a wave and ‘+’ represents the detected b wave by the proposed algorithm.

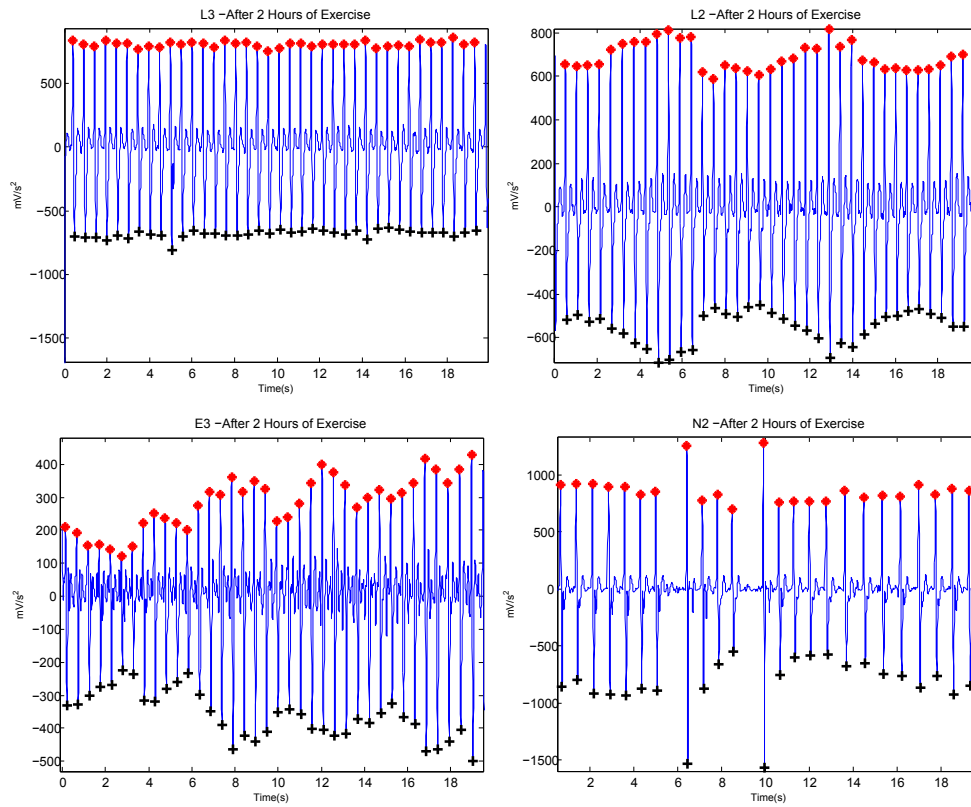


Figure 9. Detected a and b waves in APG signals after 2 hours of exercise. It contains (a) stationary signals, (b) non-stationary signals, (c) low amplitudes, and (d) irregular heart rhythm. Here, ‘*’ represents the detected a wave and ‘+’ represents the detected b wave by the proposed algorithm.

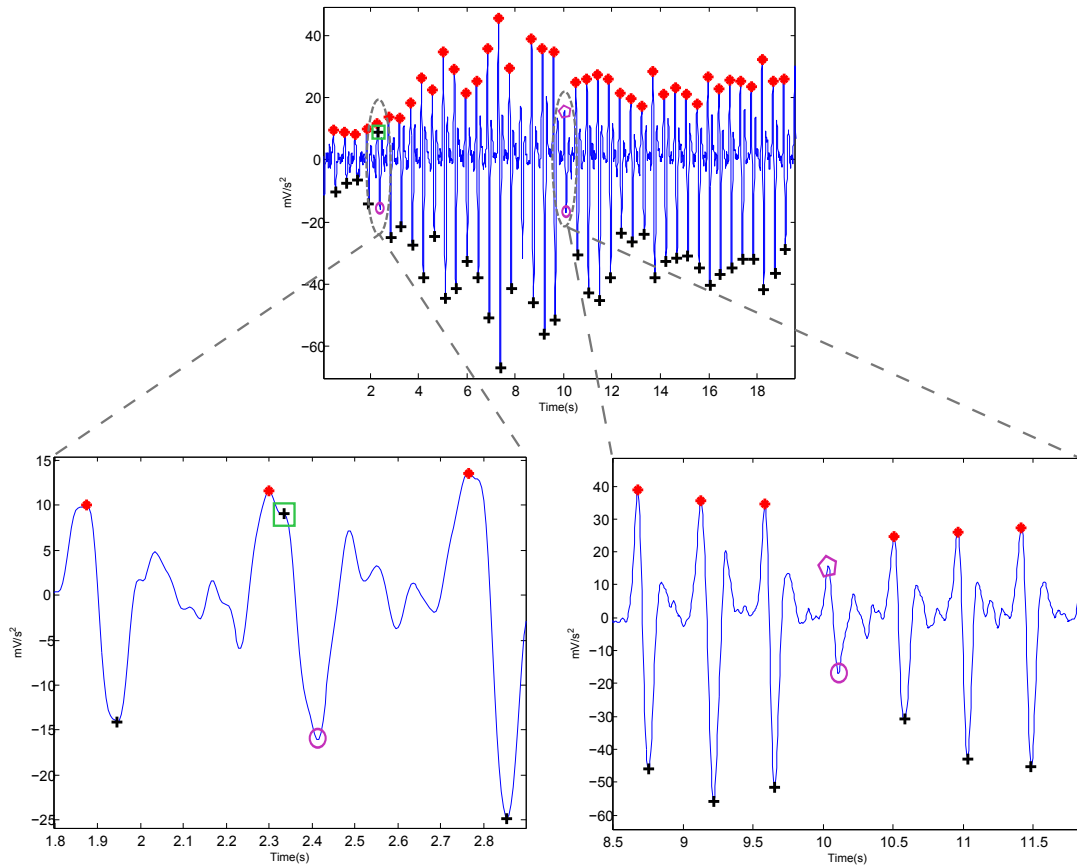


Figure 10. Instances of failure occurring with the proposed algorithm (subject: A1 after 2 hours of exercise). Here, ‘*’ represents the detected *a* wave and ‘+’ represents the detected *b* wave by the proposed algorithm. The purple pentagon represents a false negative for the *a* wave, while purple circle represents the false negative for the *b* wave. The green square represents the false positive of the *b* wave, which was the only false positive incurred by the proposed *b* detection algorithm in the testing dataset.